Journal of Mathematical Chemistry 17 (1995) 323–333

Heterogeneous chemical kinetics: A two-dimensional insight into sigmoid α–t curve

A.Korobov

Kharkov University, P.O.Box 10313, Kharkov 310023, Ukraine

Received 20 April 1993; revised 6 October 1994

In discussing the interrelation between the wide variety of heterogeneous chemical reactions and the constant form of conventional kinetic $\alpha(t)$ and $\vec{\alpha}(t)$ experimental curves, these curves are constructed in terms of 2D Dirichlet tessellations. In mathematical respect the result is the possibility to indicate 11 singular points on each curve, providing a more detailed treatment of experimental data. In chemical respect this enables one to take the diversity of crystal structures and chemical interactions into account.

1. Geometrical universality vs. chemical variety

One of the central problems of the (bulk) heterogeneous chemical kinetics in theoretical respect is the failures in model discrimination not infrequently occurring in the course of IKP (inverse kinetic problem) solution [1]. When these failures are discussed in the context of "diagnostic limits" [2] of conventional models, a striking contrast between a wide variety of heterogeneous reactions and practically always sigmoid form of the experimental "degree of conversion α–time t" curve attracts attention as one of the points at issue. This constancy of sigmoid form has to a degree determined the modern geometric-probabilistic approach [3–7] to heterogeneous chemical kinetics through giving birth to the idea of some universal geometrical regularities of nuclei formation and growth.

The idea of nuclei was borrowed from biology [8] soon after the basic work of Langmuir [9] had appeared. Along with this it was noted that whatever the chemical nature of a reaction, the corresponding kinetic $\alpha(t)$ curve is practically always sigmoid, i.e. the only type of kinetic curve corresponding to various types of chemical reactions. (In this respect, $\alpha(t)$ and $\vec{\alpha}(t)$ curves, sketched in fig. 1, may well serve as a symbol of heterogeneous chemical kinetics, or at least of the problems of IKP solution, and the final aim of the present paper is to construct such curves within the suggested approach.) In addition it appeared that $\alpha(t)$ curves obtained for reactions essentially different in chemical nature may be quite similar, whereas $\alpha(t)$

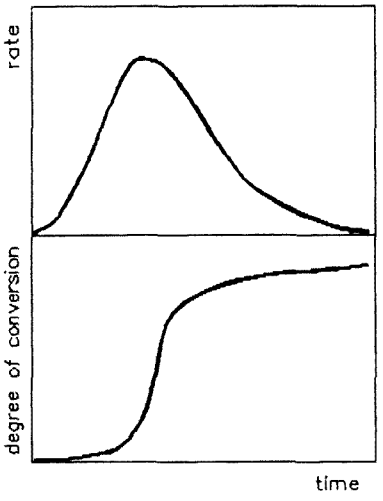

Fig. 1. Typical form of $\alpha(t)$ and $\bar{\alpha}(t)$ curves.

curves obtained for similar reactions may be quite different [10]. This has led to the idea that some universal geometrical regularities of nuclei growth are superimposed on the chemical regularities and mask them, thus determining the shape and similarity of $\alpha(t)$ curves.

The probabilistic aspect appeared in connection with the necessity to take into account the impingement of randomly distributed growing nuclei. This problem has been solved in terms of geometrical probabilities by Kolmogorov [11] and Mehl and Johanson [12] practically at the same time. Later Avrami suggested a combinatorial interpretation [13]. These classical works gave birth to the geometric-probabilistic scheme, on which the experimental data interpretation is based in modern heterogeneous chemical kinetics. (Diffusive models are not considered here.)

To discern the wide chemical variety remaining within the geometric-probabilistic scheme, the solid reagent must be represented in mathematical models as a chemical individual, i.e. with the account of its crystal structure [1]. This necessitates the restatement of the scheme in terms of tessellations and determines a two-dimensional approach [14]. The simultaneous use of two varieties of Dirichlet tessellations, planigons and random mosaics, enables one to discuss both chemical and geometrical aspects of the problem in one and the same mathematical terms [15]. In the case of p1 symmetry group, when planigons and Wigner–Seitz cells coincide, this may be done in the following way.

(i) The nucleus growth is represented with taking into account the chemical individuality of a solid reagent in terms of planigons [16,17]. A single crystal face is considered as a packing of planigons (fig. 2(a)) and plays the role of a chemical individual [15]. An occasional activation of one of the surface centers leads to the increase of reactivity of the immediate neighbors, which in this context are the centers of action of planigons having common edges with this one. As a result, at the

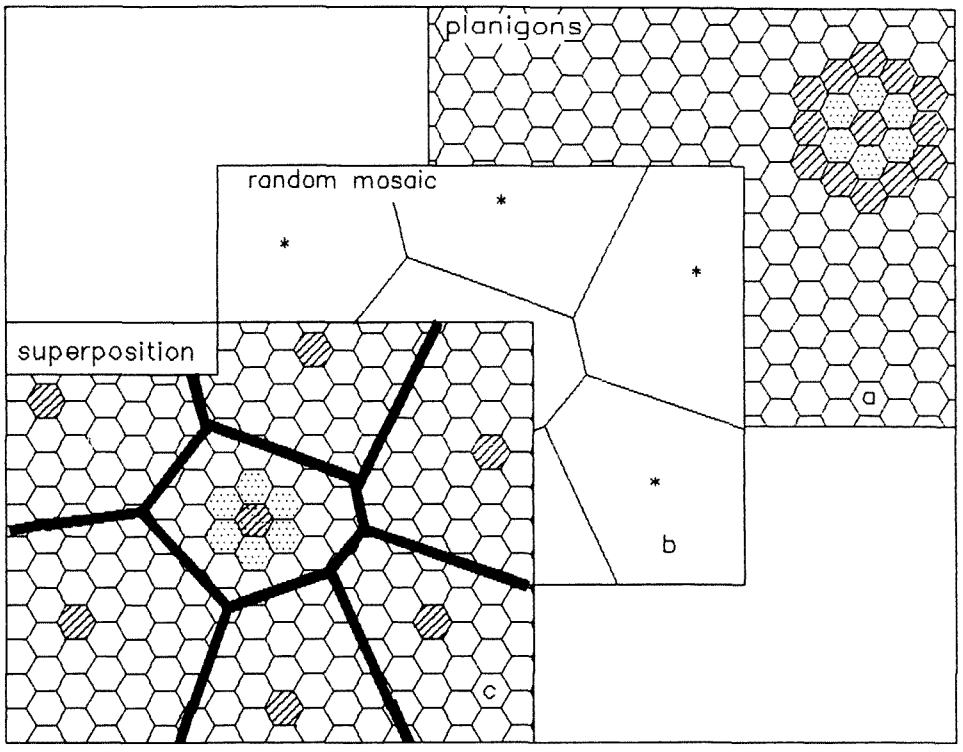

Fig. 2. Two-dimensional heterogeneous chemical reaction in terms of Dirichlet domains: (a) nucleus growth in terms of planigons; (b) nuclei appearance in terms of random mosaics; (c) superposition of two types of Dirichlet domains.

first step (representing in this case a discrete time) reaction "propagates" onto this neighboring planigons. We will say that these planigons "have entered into reaction". We will consider the next surrounding as a reaction zone (in fig. 2(a) it is shown by dots). It consists of planigons that will enter into reaction at the next step, etc.

(ii) The nuclei appearance is represented in terms of random mosaics [18], which means a spatial rather than purely temporal representation (fig. 2(b)). Each cell of this mosaic is the "rightful domain" of its nucleus and will be filled by it in the long run. The random mosaic as a whole is characterized by its averaged random cell which is always a hexagon [18]. Such a hexagon is sketched in the central part of fig. 2(c). The random mosaic remains invariable only if the number of nuclei is constant. The appearance of new nuclei in the course of a process leads to its rearrangement. As a result, the averaged hexagon cell, characterizing this mosaic, is decreased.

(iii) For representing nuclei impingements these both types of Dirichlet tessellations are superimposed resulting in the following picture (fig. 2(c)): an ever decreasing random hexagon cell with an ever increasing nucleus, consisting of planigons,

inside it. Nuclei impingements are simulated by the "impingements" of the growing nucleus with edges of the averaged cell. The rate of cell decrease is determined by the intensity of nuclei formation, whereas the rate of nucleus growth is determined by the rate of reaction front evolution [15].

The peculiar feature of this model representation, as will be shown in the next section, is the linearity of unrestricted nucleus growth. The discussed sigmoid form of $\alpha(t)$ curves will be considered as a deviation from this linearity because of nuclei impingements. As a result we will not only get a deeper insight into its structure but also sketch the way of an adequate algebraic representation.

2. Unrestricted growth: Linearity

The linearity of unrestricted growth may be shown in the most natural way using graph representation. That planigons, which have common edges with the growing figure, are added to it at each "step" (since the nearest neighbors are separated by the edges and not by the vertexes). For quadrangle planigons this is sketched in fig. 3. The corresponding graph is closed. It would be convenient to draw it on a cylinder; on the plane figure the right and left points are the same, which is shown by dotted lines. Since the evolution is concerned, it is natural to consider this graph as the oriented one. The corresponding nonoriented graph is homogeneous: $\rho(a) = 4$ for all vertexes ($\rho(a)$ is the local degree of the vertex a).

The graph vertexes fall into nonintersecting subsets with respect to their dis-

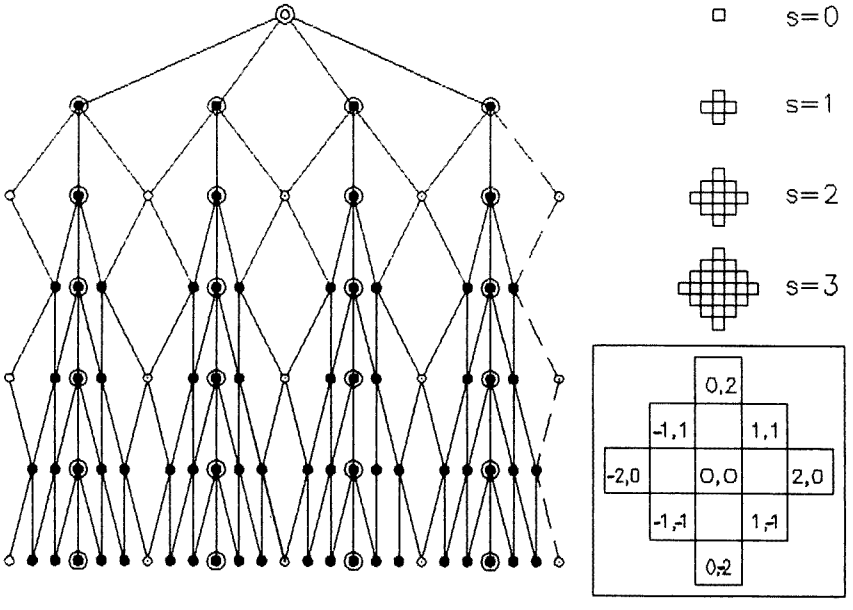

Fig. 3. Graph representation of nucleus growth (s is the step number).

tances from the center of the graph. Each of these subsets corresponds to the definite step s; in fig. 3, corresponding vertexes are situated in the same horizontal "row". It is convenient to count s off zero.

The oriented graph has (apart from its center) three types of vertexes ($\rho(a)$ and $\rho^*(a)$ are the numbers of incoming and outgoing edges, respectively):

(a) $\rho(a) = 3$, $\rho^*(a) = 1$; in fig. 3 they are shown by solid circles inside empty ones. There are 4 vertexes of this type at each step (in each horizontal "row"). So, they do not multiply.

(b) $\rho(b) = 2$, $\rho^*(b) = 2$, and each vertex of this type is linked directly with two vertexes of type (a), belonging to the previous "row"; in fig. 3 they are shown by empty circles. Only "rows" with even s contain vertexes of this type; in this case there are always 4 vertexes in a "row". So, they as well do not multiply and, in addition, oscillate.

(c) $\rho(c) = 2$, $\rho^*(c) = 2$, and each vertex of this type is linked directly with only one vertex of type (a); in fig. 3 they are shown by solid circles. Their number is increased by 8, but only at even s.

Thus, four vertexes (four planigons) are added at each step, and the process under discussion may be described by a simple arithmetic progression with first term zero and difference $d = 4$:

$$\vec{\alpha}(s) = 4s\,. \tag{1}$$

This constant growth is due to the following mechanism. The number of vertexes of type (a) remains invariable at each step. In passing from even s to odd s, the number of vertexes of type (c) increases by 8. But along with this 4 vertexes of type (b) are "switched out", compensating this surplus increase. In passing from odd s to even s, the number of vertexes of type (c) remains constant, but this is compensated by "switching on" 4 oscillating vertexes of type (b).

For describing the restricted growth we will also need the following combinatorial interpretation. A coordinate system may be naturally connected with the growing figure (see the inset in fig. 3). This enables one to describe the growth process by the simple condition

$$|x| + |y| = s\,. \tag{2}$$

This condition is satisfied by (x, y) pairs consisting of the very first and very last terms of the set $\{0, 1, 2, \ldots, s\}$, the second and penultimate terms, etc. For even s the number of different pairs $(x \leqslant y)$ is $n_e = s/2 + 1$ (e.g. $s = 4$: (0,4); (1,3); (2,2)); for odd s $n_o = (s+1)/2$ (e.g. $s = 5$: (0,5); (1,4); (2,3)). In both cases there is only one pair containing zero, for which only one sign alternation is possible. For other pairs there are four possibilities (e.g. (1,4); (−1,4); (1,−4); (−1,−4)). Taking this into consideration, one gets $n'_e = 4(s/2) + 2 = 2s + 2$ and $n'_o = 4((s+1)/2 - 1) + 2 = 2s$. Further, x and y may be replaced. Except for the case of $x = y$ (for even s),

this doubles the number of (x, y) pairs. And finally one arrives at (1) for both even and odd step numbers.

In this way it is not difficult to check that the obtained result is true also for hexagonal planigons. At each step s the number of planigons in the reaction zone increases by ν:

$$\vec{\alpha}(s) = \nu s\,, \tag{3a}$$

$$\alpha(s) = \nu s^2/2 + 1\,, \tag{3b}$$

where the number of planigon edges ν may be either 4 or 6, and s is counted off zero). These relationships describe the unrestricted growth.

Keeping in mind that the modern formalism of heterogeneous chemical kinetics is the formalism of differential equations, note also the possibility of describing the process under discussion in terms of (second-order) difference equations:

$$\mathbf{u}_s = A^s \mathbf{u}_0\,, \tag{4a}$$

$$\vec{\alpha}(s) = \mathbf{u}_s(2)\,, \tag{4b}$$

where $\mathbf{u}_0 = (\vec{\alpha}(0), \vec{\alpha}(0) + d)$, $\mathbf{u}_s = (\vec{\alpha}(s), \vec{\alpha}(s+1))$, $A = \left[\begin{smallmatrix} 0 & 1 \\ -1 & 2 \end{smallmatrix}\right]$.

Therefore, the rate of unrestricted growth is linear independently of the planigon sort. This feature of the suggested model is in agreement with experimental observations: it is often mentioned in the literature on the subject (see, for instance, [4,6]) that at the beginning stages of a process the rate is linear. But in the context of the essential nonlinearity of chemical kinetics (succinctly described by Benson [19]) this leads us to the question in what particular way the restriction of growth determines this nonlinearity.

3. Restricted growth: Singular points

Now we are in a position to describe the sigmoid form of $\alpha(t)$ curve in terms of Dirichlet tessellations as a result of nuclei impingements.

Within the suggested approach the impingements of a nucleus with neighboring nuclei are simulated as its impingements with the edges of the averaged hexagon cell. To start with, consider the case of a single straight line. No difficulties arise provided that this line is parallel to one of the axis of the growing nucleus (fig. 4(a)). Arguments similar to those in section 2 show that the increase of planigon number in the reaction zone is also described by second-order difference equations similar to (4a), but with $d = 2$. The first term $\vec{\alpha}(0)$ in this case is different from zero and is determined by the boundary condition, i.e. by the number of planigons in the reaction zone at the very first step of restricted growth. The impingement of the nucleus with the straight line results in the appearance of a salient point on the $\vec{\alpha}(s)$ graph: linearity is reserved and the slope is halved. In fig. 4(a), parts A and B correspond

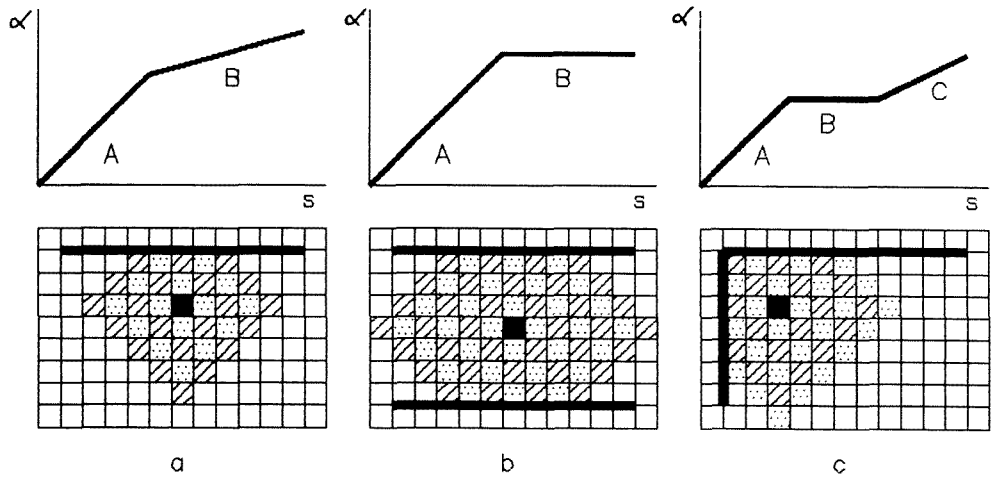

Fig. 4. The simplest examples of restricted growth: (a) the only restricted line; (b) two parallel restricted lines; (c) two perpendicular restricted lines.

to unrestricted and restricted growth, respectively. Later we will see that actually the picture is a bit more involved.

Similarly one may check that two parallel restricted lines provide the stationary growth with $d = 0$ (fig. 4(b)), whereas two perpendicular lines give the short interval of stationary growth (part B in fig. 4(c)) followed by the increase with $d = 1$ (part C). This gives one the initial idea as to the way the $\alpha(s)$ curve will be constructed.

But if the restricted line is situated at an angle to the axis of the growing figure, one faces considerable difficulties. The most simple way to illustrate them is as follows.

Until the growing nucleus is considered as a spherical one and the plane is believed to have no structure, the impingement of this nucleus with the edge of a hexagon cell means that there is a similar nucleus on the other side and at the same distance from this edge (fig. 5(a)). First these two nuclei impinge in the single point situated on the edge. Then the boundary between them propagates along the edge. Just in this sense we said that the growing nucleus impinges with the edge of the averaged cell.

In terms of planigons the complete analogy may be kept only if the restricted edge is parallel to one of the axis of the growing figure (fig. 5(b)). In the general case, two adjacent growing nuclei impinge not along the straight line but along the stepwise boundary formed by the "chain" of planigons (fig. 5(c)). The number of these planigons is equal to the number of shortest distances between two centers of action in the M metric determined by a particular planigon sort.

Figure 5(d) shows this boundary in our case. It separates planigons situated closer to one of the centers of action (solid hatching) from planigons situated closer

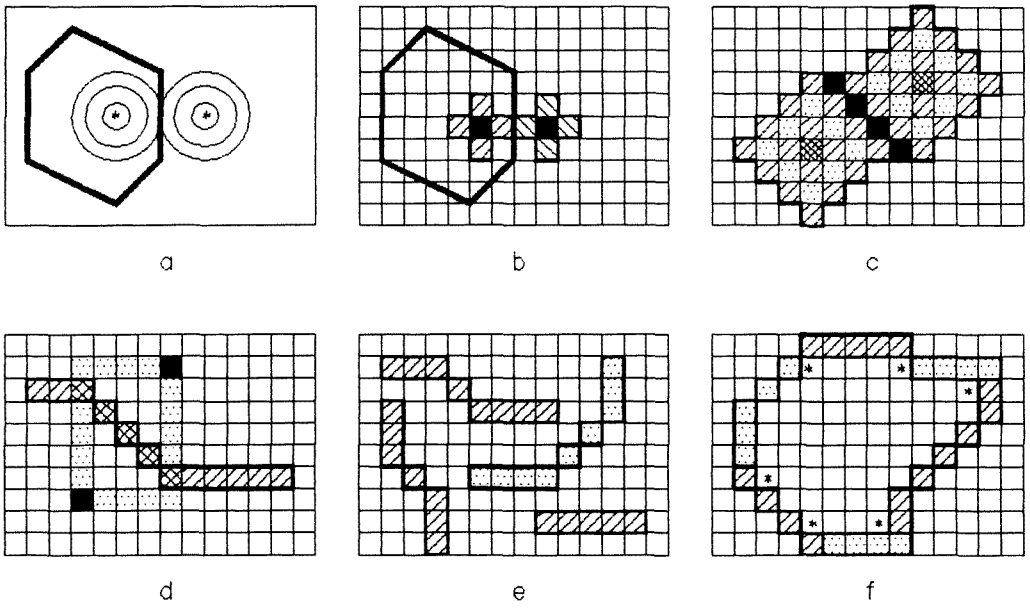

Fig. 5. Transition to the metric determined by planigons; explanations are given in the text.

to another center of action. In other words, this boundary is nothing else than the geometric locus consisting of planigons being equidistant from two centers of action. Each of these centers may be chosen as the origin of the coordinate system. Let it be the lower one in fig. 5(d). Note the following peculiarities of the considered boundary:

- the number of planigons in the stepwise part (double hatching) is equal to

  $$n = \min(|\Delta x|, |\Delta y|) + 1\,, \tag{5}$$

  where Δx and Δy are the distances between centers of action along corresponding axes (shown by dots);
- one of these planigons is surely situated on one of the axes, i.e. its coordinates are $(0, l)$ or $(l, 0)$ depending on $\min(|\Delta x|, |\Delta y|)$ where $l = r/2, r = |\Delta x| + |\Delta y|$;
- the stepwise part may be prolongated (ad infinitum) in both directions by straight parts, orientated along the second axis; so, the boundary as a whole is situated always in one half-plane;
- the stepwise part may degenerate into a single planigon (situated on an axis); in this particular case, we get simply a straight boundary parallel to another axis;
- to determine the boundary it is sufficient to point out two of its ends.

Thus, the boundary under discussion can have the form shown in fig. 5(e) by single hatching and cannot have the form shown by dots. Six intersecting boundaries

make up the hexagon in the M metric (fig. 5(f)). Such a hexagon restricts the nucleus growth.

Considering the nucleus growth inside the averaged hexagon in the M metric, one may follow the formation of $\vec{\alpha}(s)$ curve and the appearance of singular points on it.

In fig. 5(f) the adjacent edges of a hexagon are hatched in a different manner, and, in addition, the vertexes are marked with asterisks. Without this the positions of vertexes are not evident (see fig. 6). Our hexagon is formed by the edges of all possible types, each of them being the boundary of the corresponding Dirichlet domain. The top edge is straight, i.e. its stepwise part is degenerated. Then clockwise: again the straight boundary, stepwise boundary prolonged in both directions, straight boundary, purely stepwise boundary, and stepwise boundary prolonged in only one direction.

The nucleus growth inside the ever decreasing random hexagon is (roughly) sketched in fig. 6. The unrestricted growth is finished when the nearest hexagon edge is reached (fig. 6(a)). This determines the first discontinuity point on the $\vec{\alpha}(s)$ curve (polygonal line). In the general case there are 11 discontinuity points: 6 of them correspond to the impingements of growing nucleus with edges, and 5 to the "filling" of vertexes (i.e. angles between adjacent edges). The "filling" of the sixth (most distant) angle determines the end of a process, and the rate vanishes. Thus, in

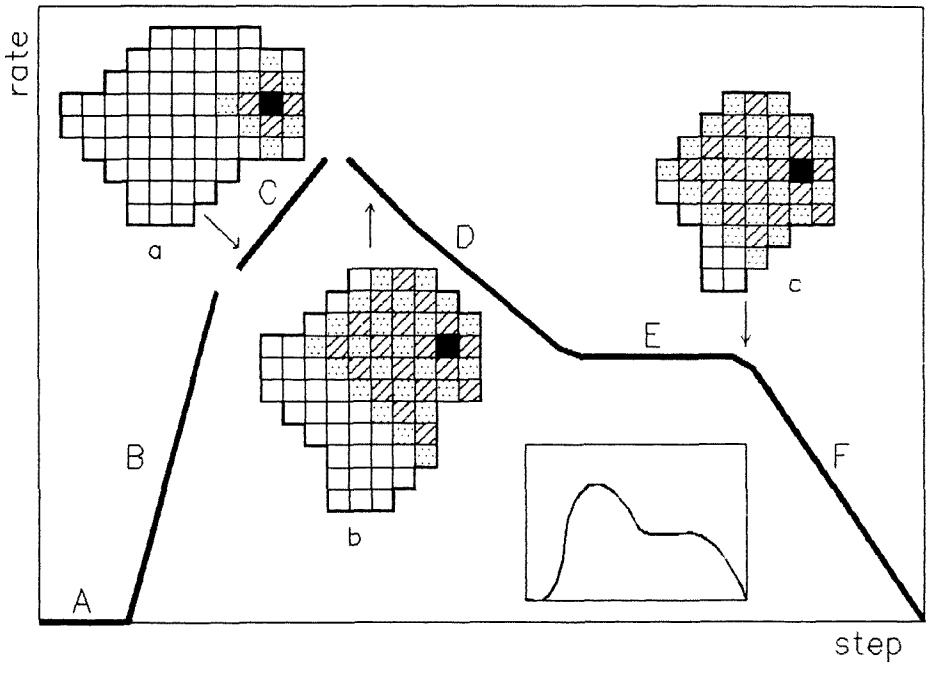

Fig. 6. "Construction" of the rate–time curve within the suggested approach; explanations are given in the text.

the general case the $\vec{\alpha}(s)$ curve consists of 12 straight units. Note, that they do not intersect, as is shown in fig. 6 for units B, C, and D. (Part A corresponds to the induction period.) In particular cases some edges and vertexes may be reached simultaneously. Accordingly, the number of discontinuity points will be less than twelve. Figure 6 shows for simplicity a particular case. Linking the separate straight units (as is shown in fig. 6 for units D, E, and F), one gets the uninterrupted polygonal line $\vec{\alpha}(s)$. Finally, after being smoothed, it assumes the form shown in the inset. Note that the maximum in this interpretation is the "freak of chance" as well as other singular points (since the hexagon is random).

As a result, reactions under discussion may be described in the general case by twelve difference equations similar to (4a), corresponding to twelve line segments of $\vec{\alpha}(s)$ curve (apart from the induction period):

$$\mathbf{u}_{\sigma}^{(j)} = A^{\sigma}\mathbf{u}_{0}^{(j)}, \tag{6}$$

where j is the consecutive number of a line segment. The step number σ in (6) is counted off the point next to the corresponding discontinuity point $s_d^{(j-1)}$: $\sigma = s^{(j)} - s_d^{(j-1)} + 1$, i.e. $\sigma = 0$ for the first point of each line segment. The value $j = 1$ corresponds to the unrestricted growth. In this case $d^{(1)}$ in $\mathbf{u}_0^{(j)} = (\vec{\alpha}^{(j)}(0), \vec{\alpha}^{(j)}(0) + d^{(j)})$ is equal to the number of planigon edges, and $\vec{\alpha}^{(1)}(0) = 0$. All discontinuity points $s_d^{(j)}$ are determined uniquely by the coordinates of hexagon vertexes. At $j > 1$ the first term $\vec{\alpha}^{(j)}(0)$ is determined by appropriate boundary conditions; $d^{(j)}$ being dependent on which edges restrict the growth at the given stage (adjacent, opposite, etc.).

4. Conclusions

(1) The constant form of $\alpha(t)$ and $\vec{\alpha}(t)$ kinetic curves reflects the universal geometrical regularities of nuclei formation, growth, and impingements that mask the basic chemical regularities. This is one of the main causes of failures in model discrimination within the conventional geometric-probabilistic approach.

(2) In terms of Dirichlet tessellations, the random nucleation and deterministic growth may be separated, and the sigmoid form of the $\alpha(t)$ curve may be represented as the deviation from linear unrestricted growth because of nuclei impingements.

(3) This enables one to indicate in the general case 11 singular points on $\alpha(t)$ and $\vec{\alpha}(t)$ curves, providing a more detailed analysis of experimental data. This number of singular points is determined by the fact that the averaged cell of a random mosaic is always a hexagon.

(4) The use of Dirichlet tessellations provides the "chemical insight" into the above geometrical universality, first of all due to a one-to-one correspondence between planigons and two-dimensional Fedorov groups (which is given in [17]). Each of 46 planigon sorts determines the corresponding metric on the plane, and in

this way the singular points may be interpreted taking into account a particular crystal structure. The biographical inhomogeneity is taken into consideration in terms of random mosaics.

(5) The possibility outlined for describing $\alpha(t)$ and $\vec{\alpha}(t)$ curves in terms of difference equations opens the way for stating the inverse kinetic problem in terms of discrete mathematics with the aim to adapt the conventional formalism of heterogeneous chemical kinetics to a more subtle simulation of chemical regularities. This point deserves separate discussion.

Acknowledgements

This work was undertaken in the Laboratory of Molecular Dynamics and Structure, Kharkov University. I would like to express my gratitude to Prof. I.V. Krivoshey for his encouragement and to Dr. S.V. Kuplevakhskij for stimulating contacts and kind help.

References

[1]] A. Korobov, J. Thermal Anal. 39 (1993) 1451.
[2] J. Šesták and J. Malek, Solid State Ionics 63–65 (1993) 245.
[3] J. Šesták, *Thermophysical Properties of Solids* (Elsevier, Amsterdam, 1984).
[4] B. Delmon, *Introduction a la Cinétique Hétérogène* (Éditions Technip, Paris, 1969).
[5] P. Barret, *Cinétique Hétérogène* (Gauthier-Villars, Paris, 1973).
[6] M.E. Brown, D. Dollimore, A.K. Galwey, *Reactions in the Solid State* (Elsevier, Amsterdam, 1980).
[7] V.Z. Belen'kiy, *Geometric-Probability Models of Crystallization* (Nauka, Moscow, 1980, in Russian).
[8] A. Macdonald and C. Hinshelwood, J. Chem. Soc. 127 (1925) 2764.
[9] I. Langmuir, J. Am. Chem. Soc. 38 (1916) 2263.
[10] D. Young, *Decomposition of Solids* (Pergamon Press, 1966).
[11] A.N. Kolmogorov, Izv. Akad. Nauk SSSR 3 (1937) 555 (in Russian).
[12] W.A. Johanson and R.F. Mehl, Trans. Am. Inst. Min. Metal. Eng. 135 (1939) 416.
[13] M. Avrami, J. Phys. Chem. 7 (1939) 1103; 8 (1940) 212; 9 (1941) 177.
[14] A. Korobov, Thermochim. Acta 243 (1994) 79.
[15] A. Korobov, Thermochim. Acta 224 (1993) 281.
[16] B.N. Delauney, Izv. Akad. Nauk SSSR 23 (1959) 365 (in Russian).
[17] B.N. Delaunay, N.P. Dolbilin and M.P. Shtogrin, Proc. Math. Inst. Acad. Sci. SSSR CXLVIII (1978) 109 (in Russian).
[18] J. Mecke and D. Stoyan, *Introduction to Stochastic Geometry* (Academie Verlag, Berlin, 1984).
[19] S. Benson, *The Foundations of Chemical Kinetics* (McGraw-Hill, 1960).